Benchmarks for electronically excited states: Time-dependent density functional theory and density functional theory based multireference configuration interaction

Mario R. Silva-Junior, Marko Schreiber, Stephan P. Sauer, and Walter Thiel

Citation: J. Chem. Phys. **129**, 104103 (2008); doi: 10.1063/1.2973541
View online: http://dx.doi.org/10.1063/1.2973541
View Table of Contents: http://jcp.aip.org/resource/1/JCPSA6/v129/i10
Published by the American Institute of Physics.

Benchmarks for electronically excited states: Time-dependent density functional theory and density functional theory based multireference configuration interaction

Mario R. Silva-Junior,[1] Marko Schreiber,[1] Stephan P. A. Sauer,[2] and Walter Thiel[1,a)]
[1]*Max-Planck-Institut für Kohlenforschung, Kaiser-Wilhelm-Platz 1, D-45470 Mülheim an der Ruhr, Germany*
[2]*Department of Chemistry, University of Copenhagen, Universitetsparken 5, DK-2100 Copenhagen, Denmark*

(Received 11 June 2008; accepted 28 July 2008; published online 10 September 2008)

Time-dependent density functional theory (TD-DFT) and DFT-based multireference configuration interaction (DFT/MRCI) calculations are reported for a recently proposed benchmark set of 28 medium-sized organic molecules. Vertical excitation energies, oscillator strengths, and excited-state dipole moments are computed using the same geometries (MP2/6-31G*) and basis set (TZVP) as in our previous *ab initio* benchmark study on electronically excited states. The results from TD-DFT (with the functionals BP86, B3LYP, and BHLYP) and from DFT/MRCI are compared against the previous high-level *ab initio* results, and, in particular, against the proposed best estimates for 104 singlet and 63 triplet vertical excitation energies. The statistical evaluation for the latter reference data gives the lowest mean absolute deviations for DFT/MRCI (0.22 eV for singlets and 0.24 eV for triplets) followed by TD-DFT/B3LYP (0.27 and 0.44 eV, respectively), whereas TD-DFT/BP86 and TD-DFT/BHLYP are significantly less accurate. The energies of singlet states with double excitation character are generally overestimated by TD-DFT, whereas triplet state energies are systematically underestimated by the currently investigated DFT-based methods. © *2008 American Institute of Physics*. [DOI: 10.1063/1.2973541]

I. INTRODUCTION

In a recent study[1] we presented an *ab initio* benchmark for electronically excited states of 28 medium-sized organic molecules with a total of 223 excitations. Calculations were performed using multistate complete-active-space second-order perturbation theory (MS-CASPT2) and coupled cluster methods (CC2, CCSD, and CC3). On the basis of these results and high-level *ab initio* data from literature, we proposed best theoretical estimates for the vertical excitation energies of 104 singlet and 63 triplet excited states.

The application of accurate *ab initio* methods such as MS-CASPT2 and CC3 is still limited in practice to rather small molecules, and there is clearly a need for reliable approximate methods that can deal with larger systems. There are a number of requirements[2] that approximate methods for electronically excited states should ideally satisfy: generality (ability to treat arbitrary types of excited states), accuracy (small errors in excitation energies, preferably less than 0.2 eV), availability of properties (including oscillator strengths, dipole moments, and analytic nuclear gradients), minimum human effort (standardization, "black-box" character, as few technical parameters as possible), and computational efficiency (small memory and CPU demand, comparable to a corresponding ground-state calculation). While none of the currently available methods fulfills all these requirements, density functional theory (DFT) is generally considered as a promising candidate. Therefore, in this article, we evaluate the performance of DFT-based approaches by comparison against our *ab initio* benchmark data.[1]

Over the past decade, time-dependent density functional theory (TD-DFT) (Ref. 3) has become one of the most prominent methods for calculating excited states.[4] A major advantage of TD-DFT is its low computational cost,[5] roughly comparable with single excitation theories based on the Hartree–Fock (HF) ground state such as configuration interaction with singles or the random phase approximation. TD-DFT excitation energies are computed as poles of the frequency-dependent density matrix response.[3] Since the commonly used adiabatic approximation represents this response in terms of single excitations, TD-DFT is best suited for excited states that are dominated by single excitations. TD-DFT properties are obtained from derivatives of the excited-state energy with respect to external perturbations.[6,7] TD-DFT calculations can be standardized and are thus user-friendly (no need to define an active space or to select reference configurations).

Evaluations of TD-DFT performance have been reported for various density functionals.[8–17] Most of these studies have compared TD-DFT vertical excitation energies either with experimental results or with published CASPT2 calculations. Generally speaking, these evaluations are less comprehensive and less systematic than desirable. The use of experimental excitation energies as reference data may be problematic because the observed band maxima do not exactly match the vertical excitation energies, bands are often found to overlap, and spectra may be available only in solution and not in the gas phase. Comparisons with published

a)Electronic mail: thiel@mpi-muelheim.mpg.de.

CASPT2 results suffer from nonuniform setup conventions in literature, e.g., with regard to geometries, basis sets, and active spaces.

An alternative DFT-based method for electronically excited states arises from the use of Kohn–Sham (KS) orbitals in a multireference configuration interaction (MRCI) framework.[18] In this ansatz, the major part of dynamic electron correlation is captured by the KS-DFT treatment, and static correlation effects are introduced by the MRCI technique, which is also flexible enough to properly describe states with double excitation character. The DFT/MRCI configuration state functions are built from KS rather than from HF orbitals. The usual HF-based MRCI formalism is formally retained, but modified by incorporating five universal empirical parameters in order to alleviate problems with the double counting of dynamic electron correlation. The five DFT/MRCI parameters have been fitted to experimental data for ten reference molecules.[18,19] Optimized values are available for singlet and triplet multiplicities[18] in combination with the BHLYP hybrid exchange-correlation functional.[20,21] The DFT/MRCI method has been tested for a number of organic chromophores[18,22] and applied to the simulation of gas phase UV/vis spectra (see, for example, Refs. 23–32) and CD spectra.[33] Overall, however, it has been validated and used less widely than TD-DFT, in spite of its promising performance in the cited papers.

In this article, we present a systematic assessment of TD-DFT (BP86, B3LYP, and BHLYP functionals) and DFT/MRCI. We use the same geometries and basis sets as in our recent *ab initio* benchmark study[1] to ensure that the results are directly comparable. This paper is structured as follows. In Sec. II we briefly describe the computational methods used. Thereafter we discuss their performance for vertical excitation energies (Sec. III A) and one-electron properties (Sec. III B). A statistical evaluation allows us to assess the merits and shortcomings of each method in more quantitative detail (Sec. III C). We conclude with a brief summary.

II. COMPUTATIONAL METHODS

All calculations were carried out at the optimized ground-state equilibrium geometries reported previously.[1,34] The TZVP basis was used throughout, which is of valence triple-ζ quality and augmented by polarization functions at all atoms.[35] As discussed before,[1] the lack of diffuse functions can compromise a balanced description of higher-lying spatially extended states. This is less relevant here, however, since the present paper focuses on the direct comparison to *ab initio* benchmark data obtained with the same basis. Further remarks on basis set dependence are found below and in literature (see, for example, Refs. 24, 27, 28, 30, and 36).

A. TD-DFT calculations

Self-consistent field (SCF) and TD-DFT calculations were performed with the TURBOMOLE program (version 5.7.1).[37] Three functionals were investigated: the gradient-corrected BP86 functional,[38,39] the hybrid Becke3–Lee–Yang–Parr (B3LYP) functional[20,38,40] with 20% of HF exchange, and the Becke-half-and-half–Lee–Yang–Parr (BHLYP) functional[20,21] with 50% of HF exchange. In the BP86 case, the resolution of identity (RI) method was employed to evaluate the two-electron integrals, making use of auxiliary basis sets from the TURBOMOLE library.[41,42] Calculations of vertical excitation energies[5,43–46] were done in the adiabatic approximation.[5,47] For every state symmetry, the energies, dipole moments, and oscillator strengths were computed for at least the five lowest states.[6,7,46,48]

It is generally accepted that TD-DFT significantly underestimates excitation energies (by up to several eV) in the case of Rydberg states[49,50] and charge transfer (CT) states,[51] because of the wrong asymptotic behavior of the standard exchange functionals. Asymptotic corrections have been suggested as a remedy for Rydberg excitation energies,[49,50] but the simultaneous description of both types of excitations remains a challenge for TD-DFT.[5,8] It should be emphasized that the current benchmark set does not include any CT states nor any "pure" Rydberg states, and is thus not designed to document the corresponding known failures of TD-DFT.

In our previous benchmark study,[1] we checked the basis set sensitivity of the computed excitation energies for ethene and formaldehyde. We found that the results converged well for the low-lying valence states, and much more slowly for the higher-lying states with partial Rydberg character where the TZVP results were several tenths of an eV above the basis set limit. It is common wisdom that DFT calculations are less sensitive to basis set extension than *ab initio* calculations, and we thus expect qualitatively similar but quantitatively less pronounced basis set effects. This has been studied for the B3LYP and BHLYP functionals through TD-DFT calculations on formamide using the correlation-consistent basis sets cc-pV*X*Z as well as the augmented variants aug-cc-pV*X*Z and d-aug-cc-pV*X*Z ($X=D,T,Q,5$).[52,53] The results are given as Supporting Information (Table VIII).[54] They confirm our qualitative expectations. The low-lying $1\,^1A''$ valence state is dominated by a single $n\rightarrow\pi^*$ excitation, and the computed excitation energies and one-electron properties converge quickly upon basis set extension: The TZVP excitation energy is within 0.1 eV of the basis set limit. On the other hand, the high-lying $2\,^1A'$ state with $\pi\rightarrow\pi^*$ character suffers from considerable valence-Rydberg mixing, and consequently its energy decreases strongly upon augmentation of the basis (by 0.7–0.9 eV when going from TZVP toward the basis set limit). We emphasize again that such variations are not of primary concern in the present context since we directly compare *ab initio* and TD-DFT results obtained with the same TZVP basis set.

B. DFT/MRCI calculations

The initial KS-DFT calculations were carried out with the TURBOMOLE program (version 5.7.1).[37] The subsequent MRCI calculations were done with the spin-free MRCI code and the associated property program,[18] which is linked to TURBOMOLE. They make use of an iterative procedure for the selection of the most important configurations. Since higher excitations (that account for dynamic correlation) are conceptually incorporated through the DFT treatment, it is justified to use an energy-based selection criterion in DFT/

MRCI and to disregard all configurations with energies above a certain configuration selection threshold. A value of 1.0 hartree yields converged results for the excitation energies and was thus adopted for all DFT/MRCI calculations. The initial reference configurations were generated from up to two (active) electrons out of ten electrons in ten active orbitals. The corresponding number of reference configurations varied between 14 for cyclopentadiene and 244 for *s*-tetrazine. The oscillator strengths were calculated in the dipole length representation. Two-electron integrals were evaluated in DFT/MRCI using the RI approximation[41,55] with the optimized RI-MP2 basis sets from the TURBOMOLE library. This standard DFT/MRCI procedure was applied to all benchmark molecules.

III. RESULTS AND DISCUSSION

Detailed results for all excited states considered are given in Tables XI–XXXIX of the Supporting Information.[54] There is one table for each benchmark molecule that contains, for each particular state, the computed vertical excitation energy, oscillator strength, and dipole moment. The present TD-DFT (BP86, B3LYP, and BHLYP) and DFT/MRCI results are supplemented with CASPT2 results from literature as well as MS-CASPT2 results, CC3 results, and the best estimates from our previous benchmark study[1] since these enter the current statistical evaluations. In addition, selected TD-DFT results from literature are given with the corresponding references.[5,8–13,56–65]

Our previous MS-CASPT2 calculations[1] were carried out with the inclusion of scalar relativistic effects in the one-electron Hamiltonian according to the Barysz–Sadlej–Snijders transformation[66] (MOLCAS option BSSM). Since such relativistic effects are not included in any of the other calculations, we have repeated all MS-CASPT2 calculations at the nonrelativistic level. In this paper, we present these nonrelativistic MS-CASPT2 results and use them throughout. As may have been expected, the differences between the nonrelativistic and relativistic MS-CASPT2 results for the current organic benchmark molecules (first-row only) are very small: The mean deviation (MD) for the vertical excitation energies of all 217 states is 0.00 eV, the mean absolute deviation (MAD) is 0.01 eV, and there are only few individual deviations of several hundredths of an eV. Some of the MS-CASPT2 excitation energies have been selected as best estimates in the case of singlet states,[1] and hence there are also some corresponding minor changes in these estimates (20 cases), which are included and used throughout this paper. In view of the tiny differences between the relativistic and nonrelativistic MS-CASPT2 results, all of our previous conclusions[1] remain valid.

A. Vertical excitation energies of the benchmark molecules

A total of 146 singlet and 71 triplet states have been evaluated; 147 of these are of $\pi \rightarrow \pi^*$ type, 67 are of $n \rightarrow \pi^*$ type, and three are of $\sigma \rightarrow \pi^*$ type. The results are listed in Tables I and II. Some notable trends are obvious at first sight: For the singlet states, BP86 gives the lowest TD-DFT excitation energies, followed by B3LYP and finally BHLYP. Due to its parametrization, DFT/MRCI gives excitation energies that generally lie between those from BP86 and B3LYP, in spite of the fact that it employs KS-BHLYP orbitals.

In the following we briefly discuss the results ordered by the class of molecules studied: polyenes; unsaturated cyclic and aromatic hydrocarbons; heterocycles; aldehydes, ketones, and amides; and nucleobases. We shall focus on comparisons with the theoretical best estimates.[1] A prerequisite for such comparisons is the correct assignment of states, which is sometimes nontrivial. Pure gradient-corrected functionals (such as BP86) give usually rather low orbital energy gaps, and hence relatively low transition energies,[44] whereas an increased admixture of HF exchange in hybrid functionals leads to blueshifted excitation energies and, occasionally, to an inversion of the states.[67] It is thus often not sufficient to make assignments by analogy, but one generally needs to check the composition of every excited-state wave function as well as one-electron properties (such as oscillator strengths) to arrive at a reliable assignment.

Ethene, butadiene, hexatriene, and octatetraene (Tables XI–XIV). The simplest chromophore studied is ethene. All DFT-based results for the singlet B_{1u} state are close to the theoretical best estimate of 7.80 eV (TD-DFT/BP86 7.73 eV, TD-DFT/B3LYP 7.70 eV, TD-DFT/BHLYP 7.69 eV, and DFT/MRCI 7.96 eV). As in the case of the *ab initio* methods (MS-CASPT2 and CC with the same TZVP basis) the DFT/MRCI result is slightly blueshifted with respect to the best estimate. The triplet state energy is generally underestimated by at least 0.2 eV, with the largest deviation of about 1 eV for TD-DFT/BHLYP.

In the series of the polyenes butadiene, hexatriene, and octatetraene, the main focus lies on the right state ordering. While the *ab initio* methods usually predict close-lying A_g and B_u states, suggesting a state switch when going from hexatriene to octatetraene, the TD-DFT calculations give a sizable separation of up to 1 eV, with the B_u state distinctly lower (3.82, 4.02, and 4.29 eV) than the A_g state (4.19, 4.84, and 5.83 eV) for all functionals. The overall performance of TD-DFT appears to be poor for these A_g and B_u states (deviations of 0.28–1.57 and 0.17–0.84 eV, respectively).

DFT/MRCI gives results for the polyenes that are much closer to the trend of the theoretical best estimates. The $2\ ^1A_g$ state (4.01 eV) is found below the $1\ ^1B_u$ state (4.25 eV) in octatetraene. The ^1A_g states show considerable double excitation character and are found relatively close to the best estimate value (maximum deviation of 0.37 eV for butadiene). To be more specific, the HOMO→LUMO double excitation contributes 26%, 32%, and 33% to the $2\ ^1A_g$ state of butadiene, hexatriene, and octatetraene, respectively, comparable with the calculated MS-CASPT2 data[1] and other published results.[68] The deviations for the triplet state energies range from −0.23 to 0.05 eV. These results are consistent with those from an extensive recent DFT/MRCI study on polyenes.[22]

Cyclopropene, cyclopentadiene, norbornadiene, benzene, and naphthalene (Tables XV–XIX). In these hydrocarbons, the largest deviations with TD-DFT (BP86) are found

TABLE I. Vertical singlet excitation energies ΔE (eV) of all evaluated molecules.

Molecule	State	CASPT2[a]	CASPT2[b]	CC3[c]	Best est.[d]	BP86	B3LYP	BHLYP	DFT/MRCI
Ethene	$1^1B_{1u}(\pi\rightarrow\pi^*)$	7.98	8.54	8.37	7.80	7.73	7.70	7.69	7.96
E-butadiene	$2^1A_g(\pi\rightarrow\pi^*)$	6.27	6.62	6.77	6.55	6.30	6.82	7.61	6.18
	$1^1B_u(\pi\rightarrow\pi^*)$	6.23	6.47	6.58	6.18	5.60	5.74	5.94	6.02
All-*E*-hexatriene	$2^1A_g(\pi\rightarrow\pi^*)$	5.20	5.42	5.72	5.09	5.07	5.69	6.66	4.92
	$1^1B_u(\pi\rightarrow\pi^*)$	5.01	5.31	5.58	5.10	4.50	4.69	4.93	4.95
All-*E*-octatetraene	$2^1A_g(\pi\rightarrow\pi^*)$	4.38	4.64	4.97	4.47	4.19	4.84	5.83	4.01
	$1^1B_u(\pi\rightarrow\pi^*)$	4.42	4.70	4.94	4.66	3.82	4.02	4.29	4.25
Cyclopropene	$1^1B_2(\pi\rightarrow\pi^*)$	7.45	7.06	7.10	7.06	6.13	6.31	6.50	6.74
	$1^1B_1(\sigma\rightarrow\pi^*)$	6.36	6.76	6.90	6.76	6.30	6.46	6.77	6.73
Cyclopentadiene	$2^1A_1(\pi\rightarrow\pi^*)$	6.31	6.31	6.61	6.31	6.09	6.52	7.23	6.15
	$3^1A_1(\pi\rightarrow\pi^*)$	7.89	8.52	8.69		8.04	8.15	8.29	8.16
	$1^1B_2(\pi\rightarrow\pi^*)$	5.27	5.51	5.73	5.55	4.93	5.02	5.15	5.42
Norbornadiene	$1^1A_2(\pi\rightarrow\pi^*)$	5.28	5.34	5.64	5.34	4.48	4.79	5.15	5.30
	$2^1A_2(\pi\rightarrow\pi^*)$	7.36	7.45	7.71		6.56	6.86	7.40	7.33
	$1^1B_2(\pi\rightarrow\pi^*)$	6.20	6.11	6.49	6.11	5.02	5.52	6.22	6.12
	$2^1B_2(\pi\rightarrow\pi^*)$	6.48	7.32	7.64		6.61	6.87	7.21	7.21
Benzene	$1^1B_{1u}(\pi\rightarrow\pi^*)$	6.30	6.42	6.68	6.54	6.00	6.10	6.15	6.31
	$1^1B_{2u}(\pi\rightarrow\pi^*)$	4.84	5.04	5.07	5.08	5.24	5.40	5.64	5.04
	$1^1E_{1u}(\pi\rightarrow\pi^*)$	7.03	7.13	7.45	7.13	6.96	7.07	7.27	7.19
	$1^1E_{2g}(\pi\rightarrow\pi^*)$	7.90	8.18	8.43	8.41	8.28	8.91	9.70	7.51
Naphthalene	$2^1A_g(\pi\rightarrow\pi^*)$	5.39	5.87	5.98	5.87	5.85	6.18	6.63	5.65
	$3^1A_g(\pi\rightarrow\pi^*)$	6.04	6.67	6.90	6.67	6.20	6.85	7.70	6.05
	$1^1B_{2u}(\pi\rightarrow\pi^*)$	4.56	4.77	5.03	4.77	4.08	4.35	4.65	4.60
	$2^1B_{2u}(\pi\rightarrow\pi^*)$	5.93	6.33	6.57	6.33	5.88	6.12	6.41	6.21
	$3^1B_{2u}(\pi\rightarrow\pi^*)$	7.16	8.17	8.44		7.53	7.87	8.45	7.84
	$1^1B_{3u}(\pi\rightarrow\pi^*)$	4.03	4.24	4.27	4.24	4.23	4.44	4.71	4.10
	$2^1B_{3u}(\pi\rightarrow\pi^*)$	5.54	6.06	6.33	6.06	5.73	5.93	6.21	5.89
	$3^1B_{3u}(\pi\rightarrow\pi^*)$	7.18	7.74	8.44		8.00	8.65	9.84	7.38
	$1^1B_{1g}(\pi\rightarrow\pi^*)$	5.53	5.99	6.07	5.99	5.04	5.58	6.28	5.53
	$2^1B_{1g}(\pi\rightarrow\pi^*)$	5.87	6.47	6.79	6.47	6.17	6.32	6.65	6.26
Furan	$2^1A_1(\pi\rightarrow\pi^*)$	6.16	6.50	6.62	6.57	6.38	6.70	7.22	6.32
	$3^1A_1(\pi\rightarrow\pi^*)$	7.66	8.17	8.53	8.13	8.16	8.25	8.43	8.21
	$1^1B_2(\pi\rightarrow\pi^*)$	6.04	6.39	6.60	6.32	6.11	6.16	6.23	6.33
Pyrrole	$2^1A_1(\pi\rightarrow\pi^*)$	5.92	6.31	6.40	6.37	6.26	6.53	6.94	6.13
	$3^1A_1(\pi\rightarrow\pi^*)$	7.46	8.17	8.17	7.91	7.85	7.96	8.15	7.88
	$1^1B_2(\pi\rightarrow\pi^*)$	6.00	6.33	6.71	6.57	6.34	6.40	6.48	6.46
Imidazole	$2^1A'(\pi\rightarrow\pi^*)$	6.72	6.19	6.58	6.19	6.29	6.45	6.65	6.29
	$3^1A'(\pi\rightarrow\pi^*)$	7.15	6.93	7.10	6.93	6.86	7.04	7.35	6.82
	$4^1A'(\pi\rightarrow\pi^*)$	8.51	8.16	8.45		8.12	8.27	8.45	8.22
	$1^1A''(n\rightarrow\pi^*)$	6.52	6.81	6.82	6.81	5.91	6.46	7.09	6.35
	$2^1A''(n\rightarrow\pi^*)$	7.56	7.90	7.93		7.18	7.45	8.16	7.63
Pyridine	$2^1A_1(\pi\rightarrow\pi^*)$	6.42	6.39	6.85	6.26	6.21	6.31	6.37	6.47
	$3^1A_1(\pi\rightarrow\pi^*)$	7.23	7.46	7.70	7.18	7.27	7.32	7.55	7.43
	$1^1B_2(\pi\rightarrow\pi^*)$	4.84	5.02	5.15	4.85	5.35	5.49	5.71	5.09
	$2^1B_2(\pi\rightarrow\pi^*)$	7.48	7.27	7.59	7.27	7.13	7.30	7.56	7.27
	$1^1B_1(n\rightarrow\pi^*)$	4.91	5.17	5.05	4.59	4.38	4.80	5.30	4.75
	$1^1A_2(n\rightarrow\pi^*)$	5.17	5.51	5.50	5.11	4.48	5.11	6.03	5.41
Pyrazine	$1^1B_{1u}(\pi\rightarrow\pi^*)$	6.70	6.89	7.07	6.58	6.41	6.50	6.55	6.71
	$2^1B_{1u}(\pi\rightarrow\pi^*)$	7.57	7.79	8.06	7.72	7.53	7.68	7.89	7.82
	$1^1B_{2u}(\pi\rightarrow\pi^*)$	4.75	4.85	5.02	4.64	5.25	5.37	5.52	4.94
	$2^1B_{2u}(\pi\rightarrow\pi^*)$	7.70	7.66	8.05	7.60	7.75	7.78	8.13	7.75
	$1^1A_u(n\rightarrow\pi^*)$	4.52	4.70	5.05	4.81	4.06	4.69	5.59	5.02
	$1^1B_{1g}(n\rightarrow\pi^*)$	6.13	6.41	6.75	6.60	5.57	6.38	7.66	6.46
	$1^1B_{2g}(n\rightarrow\pi^*)$	5.17	5.68	5.74	5.56	5.11	5.55	6.02	5.26
	$1^1B_{3u}(n\rightarrow\pi^*)$	3.63	4.12	4.24	3.95	3.59	3.96	4.40	4.00
Pyrimidine	$2^1A_1(\pi\rightarrow\pi^*)$	6.72	6.63	7.06	6.95	6.46	6.58	6.67	6.69
	$3^1A_1(\pi\rightarrow\pi^*)$	7.57	7.21	7.74		7.32	7.48	7.73	7.46
	$1^1B_2(\pi\rightarrow\pi^*)$	4.93	5.24	5.36	5.44	5.59	5.74	5.98	5.35
	$2^1B_2(\pi\rightarrow\pi^*)$	7.32	7.64	8.01		7.57	7.76	7.96	7.74
	$1^1B_1(n\rightarrow\pi^*)$	3.81	4.44	4.50	4.55	3.80	4.27	4.87	4.36

TABLE I. (*Continued.*)

Molecule	State	CASPT2[a]	CASPT2[b]	CC3[c]	Best est.[d]	BP86	B3LYP	BHLYP	DFT/MRCI
	$1^1A_2(n\rightarrow\pi^*)$	4.12	4.80	4.93	4.91	4.02	4.60	5.39	4.82
Pyridazine	$2^1A_1(\pi\rightarrow\pi^*)$	4.86	5.18	5.22	5.18	5.46	5.61	5.83	5.16
	$3^1A_1(\pi\rightarrow\pi^*)$	7.50	7.62	7.82		7.39	7.50	7.76	7.53
	$1^1B_2(\pi\rightarrow\pi^*)$	6.61	6.31	6.93		6.32	6.43	6.48	6.51
	$2^1B_2(\pi\rightarrow\pi^*)$	7.39	7.29	7.55		7.10	7.24	7.45	7.25
	$1^1A_2(n\rightarrow\pi^*)$	3.66	4.31	4.49	4.31	3.54	4.18	5.03	4.25
	$2^1A_2(n\rightarrow\pi^*)$	5.09	5.77	5.74	5.77	5.01	5.44	6.05	5.29
	$1^1B_1(n\rightarrow\pi^*)$	3.48	3.78	3.92	3.78	3.15	3.58	4.10	3.63
	$2^1B_1(n\rightarrow\pi^*)$	5.80	6.52	6.41		5.45	6.09	6.99	6.15
s-triazine	$2^1A_1'(\pi\rightarrow\pi^*)$	6.77	7.25	7.41		6.87	7.01	7.12	7.02
	$1^1A_2'(\pi\rightarrow\pi^*)$	5.53	5.79	5.71	5.79	5.95	6.14	6.45	5.70
	$1^1E'(\pi\rightarrow\pi^*)$	8.16	7.50	8.04		7.63	7.79	8.06	7.81
	$1^1A_1''(n\rightarrow\pi^*)$	3.90	4.60	4.78	4.60	3.84	4.45	5.31	4.69
	$1^1A_2''(n\rightarrow\pi^*)$	4.08	4.66	4.76	4.66	4.08	4.54	5.16	4.56
	$1^1E''(n\rightarrow\pi^*)$	4.36	4.70	4.81	4.70	3.99	4.54	5.27	4.77
	$2^1E''(n\rightarrow\pi^*)$	7.15	7.71	7.80		6.71	7.49	8.42	7.26
s-tetrazine	$1^1A_u(n\rightarrow\pi^*)$	3.06	3.51	3.79	3.51	2.86	3.51	4.40	3.70
	$2^1A_u(n\rightarrow\pi^*)$	5.28	5.50	5.46	5.50	4.60	5.04	5.60	5.05
	$1^1B_{1g}(n\rightarrow\pi^*)$	4.51	4.73	4.97	4.73	4.13	4.73	5.33	4.45
	$2^1B_{1g}(n\rightarrow\pi^*)$	5.99	6.45	6.87		5.87	6.64	7.73	6.00
	$3^1B_{1g}(n\rightarrow\pi^*)$	6.20	6.73	7.08		6.53	7.40	9.20	6.49
	$1^1B_{2g}(n\rightarrow\pi^*)$	5.05	5.20	5.34	5.20	4.79	5.29	5.80	4.75
	$2^1B_{2g}(n\rightarrow\pi^*)$	5.48	6.06	6.23		5.24	5.99	7.27	5.68
	$2^1B_{3g}(\pi\rightarrow\pi^*)$	8.12	8.34	8.47		8.72	9.30	9.96	7.44
	$1^1B_{1u}(\pi\rightarrow\pi^*)$	7.13	6.94	7.45		6.82	6.90	6.88	7.08
	$2^1B_{1u}(\pi\rightarrow\pi^*)$	7.54	7.42	7.79		7.36	7.48	7.70	7.53
	$1^1B_{2u}(\pi\rightarrow\pi^*)$	4.89	4.93	5.12	4.93	5.46	5.58	5.74	5.07
	$2^1B_{2u}(\pi\rightarrow\pi^*)$	7.94	8.14	8.51		8.09	8.26	8.57	8.26
	$1^1B_{3u}(n\rightarrow\pi^*)$	1.96	2.29	2.53	2.29	1.85	2.24	2.72	2.35
	$2^1B_{3u}(n\rightarrow\pi^*)$	6.37	6.77	6.67		5.64	6.29	7.22	6.41
Formaldehyde	$1^1A_2(n\rightarrow\pi^*)$	3.91	3.99	3.95	3.88	3.80	3.89	4.00	3.71
	$1^1B_1(\sigma\rightarrow\pi^*)$	9.09	9.14	9.18	9.10	8.80	8.89	9.09	8.76
	$2^1A_1(\pi\rightarrow\pi^*)$	9.77	9.32	10.45	9.30	9.95	9.17	9.32	9.19
Acetone	$1^1A_2(n\rightarrow\pi^*)$	4.18	4.44	4.40	4.40	4.21	4.34	4.55	4.23
	$2^1A_1(\pi\rightarrow\pi^*)$	9.16	9.31	9.65	9.40	8.76	9.04	8.97	8.53
	$1^1B_1(\sigma\rightarrow\pi^*)$	9.10	9.27	9.17	9.10	8.15	8.60	9.06	8.56
p-benzoquinone	$1^1A_u(n\rightarrow\pi^*)$	2.50	2.77	2.85	2.77	2.02	2.58	2.55	2.29
	$1^1B_{1g}(n\rightarrow\pi^*)$	2.50	2.76	2.75	2.76	1.89	2.43	3.04	2.22
	$1^1B_{1u}(\pi\rightarrow\pi^*)$	5.15	5.28	5.62	5.28	4.49	4.83	5.31	5.07
	$2^1B_{1u}(\pi\rightarrow\pi^*)$	7.08	7.92	7.82		6.82	7.25	7.73	7.60
	$1^1B_{3g}(\pi\rightarrow\pi^*)$	4.19	4.26	4.59	4.26	3.36	3.73	4.25	3.99
	$2^1B_{3g}(\pi\rightarrow\pi^*)$	6.34	6.96	7.27	6.96	6.12	6.59	7.32	6.71
	$1^1B_{3u}(n\rightarrow\pi^*)$	5.15	5.64	5.82	5.64	4.39	5.43	6.80	5.81
Formamide	$1^1A''(n\rightarrow\pi^*)$	5.61	5.63	5.65	5.63	5.46	5.55	5.77	5.47
	$2^1A'(\pi\rightarrow\pi^*)$	7.41	7.39	8.27	7.39	7.90	8.13	8.84	8.14
	$3^1A'(\pi\rightarrow\pi^*)$	10.50	10.54	10.93		10.98	10.92	11.38	10.57
Acetamide	$1^1A''(n\rightarrow\pi^*)$	5.54	5.69	5.69	5.69	5.41	5.56	5.86	5.48
	$2^1A'(\pi\rightarrow\pi^*)$	7.21	7.27	7.67	7.27	7.50	7.46	8.14	7.51
	$3^1A'(\pi\rightarrow\pi^*)$	10.08	10.09	10.50		9.42	10.01	10.59	9.98
Propanamide	$1^1A''(n\rightarrow\pi^*)$	5.48	5.72	5.72	5.72	5.43	5.59	5.89	5.47
	$2^1A'(\pi\rightarrow\pi^*)$	7.28	7.20	7.62	7.20	7.28	7.76	8.09	7.46
	$3^1A'(\pi\rightarrow\pi^*)$	9.95	9.94	10.06		8.17	9.00	10.07	9.51
Cytosine	$2^1A'(\pi\rightarrow\pi^*)$	4.39	4.67		4.66	4.20	4.64	5.19	4.62
	$3^1A'(\pi\rightarrow\pi^*)$	5.36	5.53		5.62	4.92	5.42	6.16	5.43
	$4^1A'(\pi\rightarrow\pi^*)$	6.16	6.40			6.49[e]	6.72	6.99	6.38
	$5^1A'(\pi\rightarrow\pi^*)$	6.74	6.97			6.37[f]	6.46	7.44	6.74
	$1^1A''(n\rightarrow\pi^*)$	5.00	5.12		4.87	3.79	4.76	6.21	4.86
	$2^1A''(n\rightarrow\pi^*)$	6.53	5.53		5.26	4.49	5.11	5.64	5.32
Thymine	$2^1A'(\pi\rightarrow\pi^*)$	4.88	5.06		5.20	4.60	5.00	5.48	5.18
	$3^1A'(\pi\rightarrow\pi^*)$	5.88	6.15		6.27	5.33	5.97	6.94	5.98

TABLE I. (*Continued.*)

Molecule	State	CASPT2[a]	CASPT2[b]	CC3[c]	Best est.[d]	BP86	B3LYP	BHLYP	DFT/MRCI
	$4\,^1A'(\pi\rightarrow\pi^*)$	6.10	6.53		6.53	5.85	6.31	7.03	6.42
	$5\,^1A'(\pi\rightarrow\pi^*)$	7.13	7.43			6.93	7.47	8.17	7.36
	$1\,^1A''(n\rightarrow\pi^*)$	4.39	4.95		4.82	4.09	4.70	5.30	4.48
	$2\,^1A''(n\rightarrow\pi^*)$	5.91	6.38		6.16	4.79	5.80	6.77	5.93
	$3\,^1A''(n\rightarrow\pi^*)$	6.15	6.85			5.33	6.21	7.70	6.43
	$4\,^1A''(n\rightarrow\pi^*)$	6.70	7.43			6.13	6.69	8.03	6.86
Uracil	$2\,^1A'(\pi\rightarrow\pi^*)$	5.00	5.23		5.35	4.77	5.19	5.67	5.33
	$3\,^1A'(\pi\rightarrow\pi^*)$	5.82	6.15		6.26	5.21	5.87	6.90	5.92
	$4\,^1A'(\pi\rightarrow\pi^*)$	6.46	6.74		6.70	6.01	6.50	7.21	6.56
	$5\,^1A'(\pi\rightarrow\pi^*)$	7.00	7.42			7.06	7.45	8.09	7.31
	$1\,^1A''(n\rightarrow\pi^*)$	4.54	4.91		4.80	3.97	4.63	5.27	4.41
	$2\,^1A''(n\rightarrow\pi^*)$	6.00	6.28		6.10	4.76	5.74	6.61	5.84
	$3\,^1A''(n\rightarrow\pi^*)$	6.37	6.98		6.56	5.23	6.14	7.72	6.43
	$4\,^1A''(n\rightarrow\pi^*)$	6.95	7.28			6.11	6.64	7.91	6.79
Adenine	$2\,^1A'(\pi\rightarrow\pi^*)$	5.13	5.20		5.25	4.99	5.27	5.67	4.99
	$3\,^1A'(\pi\rightarrow\pi^*)$	5.20	5.29		5.25	4.57	5.00	5.48	5.15
	$4\,^1A'(\pi\rightarrow\pi^*)$	6.24	6.34			5.84	6.32	6.87	6.29
	$5\,^1A'(\pi\rightarrow\pi^*)$	6.72	6.64			6.27	6.69	7.30	6.19
	$6\,^1A'(\pi\rightarrow\pi^*)$	6.99	6.87			6.65	7.08	7.71	7.10
	$7\,^1A'(\pi\rightarrow\pi^*)$	7.57	7.56			6.91	7.52	8.22	6.62
	$1\,^1A''(n\rightarrow\pi^*)$	6.15	5.19		5.12	4.30	4.97	5.81	5.11
	$2\,^1A''(n\rightarrow\pi^*)$	6.86	5.96		5.75	5.05	5.61	6.34	5.72

[a]Data from publications by the Roos group in the 1990s. For references, see Ref. 1.
[b]SA-CASSCF/MS-CASPT2 results using MP2/6-31G* ground-state equilibrium geometries (constrained to their highest possible symmetry) and TZVP basis set. See Ref. 1 for details.
[c]CC3 results using MP2/6-31G* ground-state equilibrium geometries (constrained to their highest possible symmetry) and TZVP basis set. See Ref. 1 for details.
[d]Theoretical best estimates for vertical excitation energies. See Ref. 1 for details.
[e]Rydberg ($n\rightarrow\sigma^*$) contamination (about 49%).
[f]Rydberg ($n\rightarrow\sigma^*$) contamination (about 59%).

for norbornadiene (−1.09 eV, $1\,^1B_2$), naphthalene (−0.95 eV, $1\,^1B_{1g}$), and cyclopropene (−0.93 eV, $1\,^1B_2$). For the B3LYP functional, the TD-DFT errors are normally in the range between −0.50 and 0.50 eV; outliers are the $1\,^1B_2$ state in cyclopropene (−0.75 eV) and the $1\,^1B_2$ state in norbornadiene (−0.59 eV). The TD-DFT/BHLYP results are more spread (−0.56 to 1.29 eV). The DFT/MRCI deviations are mostly between −0.32 and 0.05 eV, exceptions being the $1\,^1E_{2g}$ state in benzene (−0.90 eV) and the $3\,^1A_g$ state in naphthalene (−0.62 eV). A trend for slight systematic underestimation of triplet excitation energies is known both for TD-DFT and DFT/MRCI.[19]

Furan, *pyrrole*, *imidazole*, *pyridine*, *pyrazine*, *pyrimidine*, *pyridazine*, *triazine*, and *tetrazine (Tables XX–XXVIII)*. In these nine heterocyclic compounds, the singlet $\pi\rightarrow\pi^*$ states are rather close to the reference data (average deviations of −0.30, 0.02, 0.47, and −0.04 eV for TD-DFT/BP86, TD-DFT/B3LYP, TD-DFT/BHLYP, and DFT/MRCI, respectively). Large deviations are encountered in TD-DFT/BHLYP for the $1\,^1B_{1g}$ state in pyrazine (1.06 eV), the $1\,^1A_2$ state in pyridine (0.92 eV), and the $1\,^1A_u$ state in pyrazine (0.78 eV). TD-DFT/BP86 tends to underestimate the excitation energies, most strongly for the $n\rightarrow\pi^*$ states. The TD-DFT/B3LYP deviations are in the range from −0.43 to 0.43 eV, with few exceptions (0.73, 0.65, and 0.64 eV for the $1\,^1B_{2u}$ state of pyrazine and *s*-tetrazine and for the $1\,^1B_2$ state of pyridine, respectively). DFT/MRCI yields singlet $\pi\rightarrow\pi^*$ excitation energies within 0.3 eV of the theoretical best estimates, while some $n\rightarrow\pi^*$ states show larger deviations (too small by more than 0.3 eV). Triplet state energies are again almost always underestimated by all DFT-based methods.

Formaldehyde, acetone, p-benzoquinone, formamide, acetamide, and propanamide (Tables XXX–XXXV). Excitation energies for $n\rightarrow\pi^*$ and $\sigma\rightarrow\pi^*$ states from TD-DFT/BP86 and TD-DFT/B3LYP are systematically too low, while those for $\pi\rightarrow\pi^*$ states scatter considerably, with deviations ranging from −0.89 to 0.65 eV (BP86) and from −0.52 to 0.69 eV (B3LYP). TD-DFT/BHLYP, on the other hand, overestimates most excitation energies, especially of $\pi\rightarrow\pi^*$ type. DFT/MRCI is usually within −0.5 to 0.25 eV of the theoretical best estimates for all kinds of excitations, except for some high-lying states such as the $2\,^1A_1$ state of acetone (−0.87 eV) and the $2\,^1A'$ state of formamide (0.75 eV). The average deviations for $\pi\rightarrow\pi^*$ singlet states are −0.38, −0.12, 0.28, and −0.18 eV for TD-DFT/BP86, TD-DFT/B3LYP, TD-DFT/BHLYP, and DFT/MRCI, respectively. Triplet state energies are on average underestimated by TD-DFT (by about 0.6 eV for all functionals) and DFT/MRCI (by about 0.3 eV).

Cytosine, thymine, uracil, and adenine (Tables XXXVI–XXXIX). The deviations for the nucleobases are quite systematic: TD-DFT/BP86 excitation energies are strongly underestimated (on average by 0.82 eV), while the TD-DFT/BHLYP

TABLE II. Vertical triplet excitation energies ΔE (eV).

Molecule	State	CASPT2[a]	CASPT2[b]	CC3[c]	Best est.[d]	BP86	B3LYP	BHLYP	DFT/MRCI
Ethene	$1^3B_{1u}(\pi\rightarrow\pi^*)$	4.39	4.48	4.48	4.50	4.15	4.03	3.47	4.31
E-butadiene	$1^3A_g(\pi\rightarrow\pi^*)$	4.89	5.16	5.17	5.08	4.95	4.86	4.44	4.85
	$1^3B_u(\pi\rightarrow\pi^*)$	3.20	3.34	3.32	3.20	2.87	2.76	2.15	3.09
All-*E*-hexatriene	$1^3A_g(\pi\rightarrow\pi^*)$	4.12	4.31	4.32	4.15	3.98	3.92	3.50	3.96
	$1^3B_u(\pi\rightarrow\pi^*)$	2.55	2.71	2.69	2.40	2.21	2.09	1.35	2.45
All-*E*-octatetraene	$1^3A_g(\pi\rightarrow\pi^*)$	3.39	3.70	3.67	3.55	3.30	3.24	2.80	3.32
	$1^3B_u(\pi\rightarrow\pi^*)$	2.17	2.33	2.30	2.20	1.81	1.68	0.72	2.04
Cyclopropene	$1^3B_2(\pi\rightarrow\pi^*)$	4.18	4.35	4.34	4.34	3.74	3.70	3.25	4.03
	$1^3B_1(\sigma\rightarrow\pi^*)$	6.05	6.51	6.62	6.62	5.81	6.01	6.28	6.31
Cyclopentadiene	$1^3A_1(\pi\rightarrow\pi^*)$	4.90	5.11	5.09	5.09	4.82	4.75	4.38	4.78
	$1^3B_2(\pi\rightarrow\pi^*)$	3.15	3.28	3.25	3.25	2.82	2.71	2.14	3.07
Norbornadiene	$1^3A_2(\pi\rightarrow\pi^*)$	3.42	3.75	3.72	3.72	3.11	3.08	2.63	3.42
	$1^3B_2(\pi\rightarrow\pi^*)$	3.80	4.22	4.16	4.16	3.71	3.62	3.07	3.85
Benzene	$1^3B_{1u}(\pi\rightarrow\pi^*)$	3.89	4.17	4.12	4.15	3.93	3.77	3.08	4.13
	$1^3B_{2u}(\pi\rightarrow\pi^*)$	5.49	5.76	6.04	5.88	4.94	5.09	5.26	5.57
	$1^3E_{1u}(\pi\rightarrow\pi^*)$	4.49	4.90	4.90	4.86	4.60	4.70	4.79	4.69
	$1^3E_{2g}(\pi\rightarrow\pi^*)$	7.12	7.38	7.49	7.51	7.13	7.33	7.47	7.40
Naphthalene	$1^3A_g(\pi\rightarrow\pi^*)$	5.27	5.53	5.52	5.52	5.25	5.33	5.31	5.18
	$2^3A_g(\pi\rightarrow\pi^*)$	5.83	6.38	6.47	6.47	5.67	5.95	6.33	6.00
	$3^3A_g(\pi\rightarrow\pi^*)$	5.91	6.59	6.79	6.79	5.59	6.07	6.58	6.31
	$1^3B_{2u}(\pi\rightarrow\pi^*)$	3.10	3.16	3.11	3.11	2.76	2.69	2.06	2.97
	$2^3B_{2u}(\pi\rightarrow\pi^*)$	4.30	4.68	4.64	4.64	4.31	4.40	4.45	4.49
	$1^3B_{3u}(\pi\rightarrow\pi^*)$	3.89	4.25	4.18	4.18	3.81	3.95	4.06	3.93
	$2^3B_{3u}(\pi\rightarrow\pi^*)$	4.45	4.97	5.11	5.11	4.03	4.22	4.42	4.65
	$1^3B_{1g}(\pi\rightarrow\pi^*)$	4.23	4.51	4.47	4.47	4.19	4.17	3.90	4.25
	$2^3B_{1g}(\pi\rightarrow\pi^*)$	5.71	6.21	6.48	6.48	5.00	5.55	6.39	6.02
	$3^3B_{1g}(\pi\rightarrow\pi^*)$	6.23	6.64	6.76	6.76	6.30	6.56	6.85	6.41
Furan	$1^3A_1(\pi\rightarrow\pi^*)$	5.15	5.49	5.48	5.48	5.24	5.21	4.67	5.15
	$1^3B_2(\pi\rightarrow\pi^*)$	3.99	4.18	4.17	4.17	3.85	3.71	2.70	3.91
Pyrrole	$1^3A_1(\pi\rightarrow\pi^*)$	5.16	5.52	5.51	5.51	5.24	5.25	5.19	5.19
	$1^3B_2(\pi\rightarrow\pi^*)$	4.27	4.51	4.48	4.48	4.18	4.07	3.63	4.23
Imidazole	$1^3A'(\pi\rightarrow\pi^*)$	4.49	4.65	4.69	4.69	4.33	4.24	3.82	4.41
	$2^3A'(\pi\rightarrow\pi^*)$	5.47	5.74	5.79	5.79	5.39	5.44	5.33	5.43
	$3^3A'(\pi\rightarrow\pi^*)$	6.53	6.44	6.55	6.55	5.92	5.95	5.99	6.22
	$4^3A'(\pi\rightarrow\pi^*)$	7.08	7.44	7.42		6.76	6.93	7.21	7.14
	$1^3A''(n\rightarrow\pi^*)$	6.07	6.36	6.37	6.37	5.53	5.83	6.12	5.92
	$2^3A''(n\rightarrow\pi^*)$	7.15	7.51	7.51		6.35	6.86	7.81	7.32
Pyridine	$1^3A_1(\pi\rightarrow\pi^*)$	4.05	4.27	4.25	4.06	4.05	3.89	3.14	4.25
	$2^3A_1(\pi\rightarrow\pi^*)$	4.73	5.03	5.05	4.91	4.78	4.84	4.89	4.84
	$3^3A_1(\pi\rightarrow\pi^*)$	7.34	7.56	7.66		7.29	7.44	7.51	7.21
	$1^3B_2(\pi\rightarrow\pi^*)$	4.56	4.71	4.86	4.64	4.42	4.51	4.57	4.60
	$2^3B_2(\pi\rightarrow\pi^*)$	6.02	6.03	6.40	6.08	5.46	5.64	5.84	5.97
	$3^3B_2(\pi\rightarrow\pi^*)$	7.28	7.87	7.83		7.54	7.75	7.93	7.52
	$1^3B_1(n\rightarrow\pi^*)$	4.41	4.57	4.50	4.25	3.71	4.04	4.39	4.31
	$1^3A_2(n\rightarrow\pi^*)$	5.10	5.52	5.46	5.28	4.34	4.98	5.85	5.33
s-tetrazine	$1^3A_u(n\rightarrow\pi^*)$	2.81	3.28	3.52	3.52	2.52	3.10	3.76	3.50
	$2^3A_u(n\rightarrow\pi^*)$	4.85	5.04	5.03	5.03	4.00	4.43	4.99	4.84
	$1^3B_{1g}(n\rightarrow\pi^*)$	3.76	4.14	4.21	4.21	3.32	3.63	3.90	3.92
	$2^3B_{1g}(n\rightarrow\pi^*)$	5.68	6.37	6.60		5.61	6.33	7.53	6.27
	$1^3B_{1u}(\pi\rightarrow\pi^*)$	4.25	4.37	4.33	4.33	4.24	3.83	2.51	4.27
	$2^3B_{1u}(\pi\rightarrow\pi^*)$	5.00	5.40	5.38	5.38	5.12	5.24	5.36	5.26
	$1^3B_{2g}(n\rightarrow\pi^*)$	4.67	4.94	4.93	4.93	4.17	4.48	4.76	4.64
	$2^3B_{2g}(n\rightarrow\pi^*)$	5.30	5.97	6.04		4.77	5.62	6.91	5.78
	$1^3B_{2u}(\pi\rightarrow\pi^*)$	4.29	4.39	4.54	4.54	4.11	4.06	3.91	4.21
	$2^3B_{2u}(\pi\rightarrow\pi^*)$	6.81	7.08	7.36		6.42	6.63	6.94	6.94
	$1^3B_{3u}(n\rightarrow\pi^*)$	1.45	1.61	1.89	1.89	1.11	1.42	1.69	1.88
	$2^3B_{3u}(n\rightarrow\pi^*)$	6.14	6.54	6.53		5.36	5.97	6.83	6.36
Formaldehyde	$1^3A_2(n\rightarrow\pi^*)$	3.48	3.58	3.55	3.50	3.05	3.13	3.21	3.32
	$1^3A_1(\pi\rightarrow\pi^*)$	5.99	5.84	5.83	5.87	5.48	5.18	4.38	5.46
Acetone	$1^3A_2(n\rightarrow\pi^*)$	3.90	4.10	4.05	4.05	3.56	3.69	3.84	3.85

TABLE II. (*Continued.*)

Molecule	State	CASPT2[a]	CASPT2[b]	CC3[c]	Best est.[d]	BP86	B3LYP	BHLYP	DFT/MRCI
	$1\,^3A_1(\pi\rightarrow\pi^*)$	5.98	6.04	6.03	6.03	5.57	5.39	4.81	5.64
p-benzoquinone	$1\,^3A_u(n\rightarrow\pi^*)$	2.27	2.66	2.62	2.62	1.56	2.05	3.20	2.31
	$1\,^3B_{1g}(n\rightarrow\pi^*)$	2.17	2.62	2.51	2.51	1.44	1.92	2.42	2.21
	$1\,^3B_{1u}(\pi\rightarrow\pi^*)$	2.91	2.99	2.96	2.96	2.42	2.19	1.21	2.62
	$1\,^3B_{3g}(\pi\rightarrow\pi^*)$	3.19	3.32	3.41	3.41	2.59	2.68	2.44	3.09
Formamide	$1\,^3A''(n\rightarrow\pi^*)$	5.34	5.40	5.36	5.36	4.87	4.97	5.14	5.12
	$1\,^3A'(\pi\rightarrow\pi^*)$	5.69	5.58	5.74	5.74	5.20	5.13	4.93	5.42
Acetamide	$1\,^3A''(n\rightarrow\pi^*)$	5.24	5.41	5.42	5.42	4.85	5.01	5.25	5.13
	$1\,^3A'(\pi\rightarrow\pi^*)$	5.57	5.63	5.88	5.88	5.26	5.26	5.14	5.52
Propanamide	$1\,^3A''(n\rightarrow\pi^*)$	5.28	5.45	5.45	5.45	4.89	5.04	5.29	5.13
	$1\,^3A'(\pi\rightarrow\pi^*)$	5.94	5.80	5.90	5.90	5.27	5.28	5.18	5.51

[a]Data from publications by the Roos group in the 1990s cited in Ref. 1.
[b]SA-CASSCF/MS-CASPT2 results using MP2/6-31G* ground-state equilibrium geometries (constrained to their highest possible symmetry) and TZVP basis set.
[c]CC3 results using MP2/6-31G* ground-state equilibrium geometries (constrained to their highest possible symmetry) and TZVP basis set.
[d]Theoretical best estimates for vertical excitation energies. See Ref. 1 for details.

results are higher than the best estimates, especially in the case of the high-lying $1\,^1A''$ state of cytosine (1.34 eV) and the $3\,^1A''$ state of uracil (1.16 eV). TD-DFT/B3LYP and DFT/MRCI results are closer to the reference data, with deviations of less than 0.40 eV.

B. One-electron properties

Theoretical studies of electronically excited states have traditionally concentrated more on the energetics rather than on one-electron properties such as oscillator strengths and dipole moments. Only relatively few studies have addressed the convergence behavior of excited-state properties, e.g., with regard to basis set or level of theory.[5,10,59,62,64,69,70] In TD-DFT the computed oscillator strengths and excited-state dipole moments are known to depend, often quite sensitively, on the chosen functional and the basis set.[6,57,71–73] For example, the oscillator strengths of the lowest-energy $\pi\rightarrow\pi^*$ transition in benzene and substituted benzenes are well reproduced by TD-DFT only when using hybrid functionals with a significant amount of HF exchange (BHLYP) and basis sets with diffuse functions, whereas they are strongly underestimated by pure DFT functionals.[72] As a second example, we quote early TD-DFT studies of the excited-state dipole moments of furan and pyrrole that show a large variation (up to several Debye) with the chosen functional and basis set,[57] as well as a strong sensitivity to approximations such as neglecting orbital relaxation in the one-particle density matrix.[73]

In analogy to the excitation energies (see Sec. II A) we have checked the basis set convergence of the computed one-electron properties at the TD-DFT level for formamide. The corresponding B3LYP and BHLYP results are documented in Table VIII of the Supporting Information.[54] As expected, we find smooth convergence for the $1\,^1A''$ state, which is dominated by a single $n\rightarrow\pi^*$ excitation with a weight of typically more than 90%: The oscillator strength is always close to zero, and the excited-state dipole moment decreases monotonically along the series of (augmented) correlation-consistent basis sets over a range of about 0.2 D to arrive at converged values of 2.4 D (TD-DFT/B3LYP) and 2.2 D (TD-DFT/B3LYP). By contrast, the $2\,^1A'$ state shows considerable valence-Rydberg mixing, and the relative weights of the $\pi\rightarrow\pi^*$ and the Rydberg excitation vary strongly with the basis set and the amount of HF exchange in the functional: The oscillator strengths are reduced by about a factor of 2 upon basis set extension and seem to converge toward a value around 0.17, while the computed excited-state dipole moments scatter irregularly (see Table VIII). These data on formamide serve as a reminder that the one-electron properties currently calculated with the TZVP basis cannot in general be considered as converged with regard to basis set extension (especially not for the higher-lying excited states). We note again, however, that this deficiency is less relevant at present since our primary objective is the direct comparison between *ab initio* and DFT results obtained with the same TZVP basis; best estimates of excited-state one-electron properties are not yet available for our benchmark set.[1]

Table IX (see Supporting Information[54]) collects published *ab initio* oscillator strengths (range of values and CASPT2 data), our own MS-CASPT2, CC2, and CCSD values, and the present TD-DFT and DFT/MRCI results for all dipole-allowed vertical transitions. The majority of computed TD-DFT and DFT/MRCI oscillator strengths are in the range of the published *ab initio* values. It is obvious that most of the TD-DFT oscillator strengths (more than 85%) increase in the sequence BP86<B3LYP<BHLYP. This is due to the increased amount of HF exchange, which leads to larger f values.[72] For weak transitions ($n\rightarrow\pi^*$ states) such trends are not visible, of course, since the oscillator strengths are close to zero in all methods. Order-of-magnitude discrepancies between individual results from different methods are found only rarely ($1\,^1B_2$ state of pyridazine, $1\,^1B_{1u}$ state of *s*-tetrazine, and $2\,^1A'$ and two higher-lying $\pi\rightarrow\pi^*$ states of adenine); in these cases the MS-CASPT2 oscillator strengths deviate from the other CC- and DFT-based results because of state contamination.

Table X (see Supporting Information[54]) summarizes the calculated ground-state and excited-state dipole moments

(TD-DFT and DFT/MRCI), and also includes our MS-CASPT2/TZVP results as well as published CASSCF data (see Ref. 34 for details). Despite many differences in the setup (with regard to basis set, active space, and geometry), there are only relatively few strong deviations between our MS-CASPT2/TZVP and the earlier CASSCF results: Deviations of more than 1 D are mainly found for states with strong configurational mixing, for example, the 1 $^1A_2$ state of norbornadiene (1.64 D), the 2 $^1A'$, 3 $^1A'$, 4 $^3A'$, and 2 $^3A''$ states of imidazole (1.26, 1.82, 1.83, and 3.04 D, respectively), as well as some high-lying $\pi \rightarrow \pi^*$ states and most of the $n \rightarrow \pi^*$ states of the nucleobases (up to 5 D).

The current DFT-based calculations employ the same basis sets and geometries as the MS-CASPT2/TZVP calculations, but still yield rather different excited-state dipole moments that show quite a large spread, with strong deviations appearing throughout the whole benchmark set. For example, compared to the MS-CASPT2 reference values, much too low dipole moments are computed for the 3 $^3A_1$ state of pyridine (0.12 D, TD-DFT/B3LYP), the 2 $^1B_2$ state of pyrimidine (0.35 D, TD-DFT/B3LYP), the 4 $^1A'$ and 5 $^1A'$ states of cytosine (3.60 and 2.19 D, TD-DFT/BP86 with strong Rydberg contamination), and the 1 $^1A''$ state of adenine (0.38 D, TD-DFT/B3LYP, an $n \rightarrow \pi^*$ state unlike the preceding cases). Generally speaking, the largest deviations from the MS-CASPT2 reference data are again found for the nucleobases (see Sec. III C 4 for more details). Of course, there are also many states (especially the low-lying ones) with much better agreement. An example is the 1 $^1A_2$ state of formaldehyde, where all theoretical values [1.39, 1.46, 1.65, 1.63, 1.57, and 1.53 D for CASSCF,[74] MS-CASPT2/TZVP, TD-DFT (BP86, B3LYP, and BHLYP), and DFT/MRCI, respectively] deviate by less than 0.20 D from the experimental value of 1.57 D.[75]

TABLE III. TD-DFT and DFT/MRCI deviations of vertical excitation energies (in eV) for singlet excited states with respect to *ab initio* reference data.

	Method			
	BP86	B3LYP	BHLYP	DFT/MRCI
Published CASPT2 results[a]				
Count[b]	146	146	146	146
Mean	−0.27	0.10	0.65	0.02
Abs. mean	0.44	0.37	0.73	0.29
Std. dev.	0.58	0.48	0.90	0.39
Max. (+) dev.	0.82	1.47	3.00	0.79
Max. (–) dev.	2.04	1.42	0.95	1.37
MS-CASPT2/TZVP results[c]				
Count[b]	146	146	146	146
Mean	−0.48	−0.11	0.44	−0.19
Abs. mean	0.56	0.30	0.52	0.26
Std. dev.	0.68	0.38	0.67	0.33
Max. (+) dev.	0.63	1.05	2.47	0.75
Max. (–) dev.	1.77	0.94	0.85	0.97
CC3/TZVP results[c]				
Count[b]	116	116	116	116
Mean	−0.61	−0.29	0.20	−0.39
Abs. mean	0.65	0.39	0.44	0.39
Std. dev.	0.73	0.46	0.57	0.46
Max. (+) dev.	0.34	0.82	2.12	—
Max. (–) dev.	1.89	1.28	1.13	1.26
Theoretical best estimates[c]				
Count[b]	104	104	104	104
Mean	−0.44	−0.07	0.43	−0.13
Abs. mean	0.52	0.27	0.50	0.22
Std. dev.	0.62	0.33	0.62	0.29
Max. (+) dev.	0.65	1.02	1.73	0.75
Max. (–) dev.	1.37	0.75	0.56	0.90

[a]Data from publications by the Roos group in the 1990s cited in Ref. 1.
[b]Total number of states considered.
[c]See Ref. 1.

C. Statistical evaluation

In the statistical evaluation for our benchmark, the present DFT-based results are related to four sets of reference data that have been assembled in our previous study: the earlier CASPT2 results from the Roos group, our own MS-CASPT2/TZVP and CC3/TZVP data, and our proposed theoretical best estimates.

1. Singlet state energies

Table III summarizes the statistical evaluation for the singlet excited states in the benchmark. Given are the number of states considered, the mean deviation (MD), the mean absolute deviation (MAD), and the standard and maximum deviations among each set. The number of states differs somewhat between the different reference sets: Available are 146 singlet state energies from the published CASPT2 and our MS-CASPT2 calculations, but only 116 CC3 energies and 104 theoretical best estimates.[1]

When using the published CASPT2 data as reference, DFT/MRCI gives the lowest MAD (0.29 eV), followed by TD-DFT/B3LYP (0.37 eV), TD-DFT/BP86 (0.44 eV), and TD-DFT/BHLYP (0.73 eV). Positive (negative) MDs indicate that the calculated energies tend to be blueshifted (redshifted) with respect to the reference values. The DFT/MRCI results (MD of 0.02 eV) thus scatter around the literature CASPT2 data. The excitation energies from TD-DFT/BP86 are lower on average (MD of −0.27 eV), while those from TD-DFT/B3LYP and TD-DFT/BHLYP are slightly and considerably higher on average (MDs of 0.10 and 0.65 eV, respectively). The largest deviations for the four DFT-based methods are found for the 1 $^1A''$ state of *s*-triazine (0.79 eV, DFT/MRCI), the 3 $^1B_{3u}$ state of naphthalene (0.82 eV, TD-DFT/BP86; 1.47 eV, TD-DFT/B3LYP), and the 3 $^1B_{1g}$ state of *s*-tetrazine (3.00 eV, TD-DFT/BHLYP), the latter marking the biggest deviation overall.

The singlet excitation energies from the MS-CASPT2 and CC3/TZVP calculations are on average about 0.2 and 0.4 eV higher than the published CASPT2 values.[1] Changing the reference set to MS-CASPT2/TZVP and CC3/TZVP will thus cause corresponding shifts in the MDs of the TD-DFT and DFT/MRCI results (Table III). Now the DFT-based excitation energies appear generally redshifted with regard to the *ab initio* data, except for TD-DFT/BHLYP. The TD-DFT/BP86 results show the worst agreement with the reference data (MDs of −0.48 and −0.61 eV compared to MS-

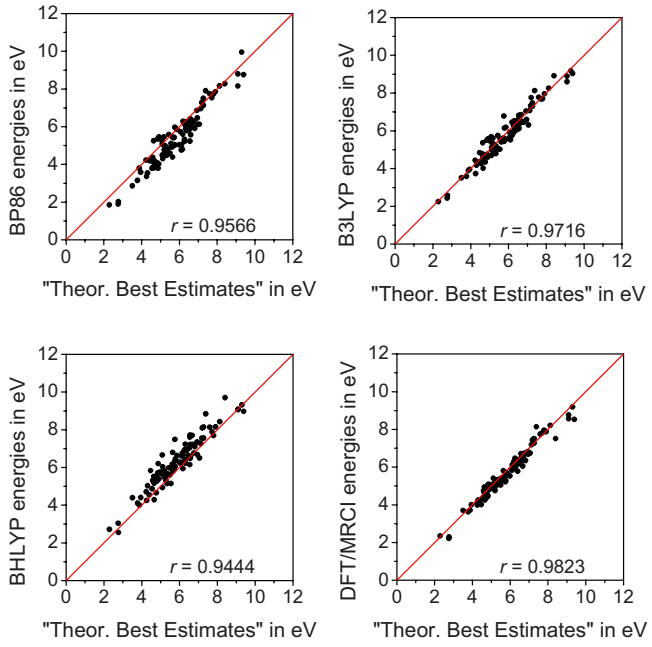

FIG. 1. (Color online) Correlation plots for all calculated singlet excited states: TD-DFT (BP86, B3LYP, and BHLYP) and DFT/MRCI vs theoretical best estimates for vertical excitation energies.

CASPT2 and CC3, respectively), whereas TD-DFT/B3LYP and DFT/MRCI perform similarly well.

The most relevant comparisons involve the theoretical best estimates as reference data. The correlation plots in Fig. 1 show immediately that TD-DFT/B3LYP and DFT/MRCI outperform TD-DFT/BP86 and TD-DFT/BHLYP. They indicate a slight edge for DFT/MRCI where the excitation energies have a smaller spread with respect to the best estimates. This is borne out by the statistical data: The MAD is smallest for DFT/MRCI (0.22 eV) followed rather closely by TD-DFT/B3LYP (0.27 eV) and much ahead of TD-DFT/BP86 (0.52 eV) and TD-DFT/BHLYP (0.50 eV). Both DFT/MRCI and TD-DFT/B3LYP tend to give singlet excitation energies that are slightly too low (MDs of −0.13 and −0.07 eV).

Figure 2 shows separate histograms for the deviations between TD-DFT/B3LYP/TZVP and theoretical best estimates of singlet $n \rightarrow \pi^*$ (left) and $\pi \rightarrow \pi^*$ (right) excited states. It is evident that there is closer agreement for the $n \rightarrow \pi^*$ states. Similar distributions are also found for the other functionals, though redshifted for TD-DFT/BP86 and blueshifted for TD-DFT/BHLYP.

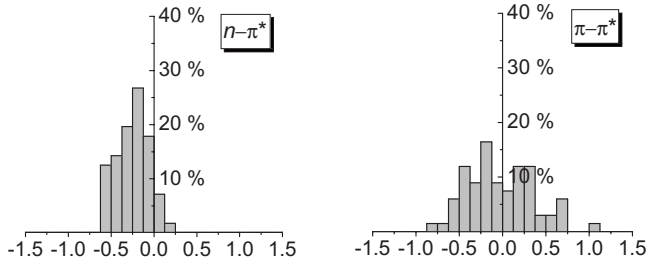

FIG. 2. Histogram of the frequency of deviation (TD-DFT/B3LYP/TZVP vs theoretical best estimates, in %) in the calculated vertical excitation energies (eV) for the singlet $n \rightarrow \pi^*$ (left) and $\pi \rightarrow \pi^*$ (right) excited states.

2. Triplet state energies

Statistical results for the triplet states are listed in Table IV and visualized in Fig. 3. The number of states considered varies for the different reference sets: 71 states are available from the earlier CASPT2 as well as from the recent MS-CASPT2 and CC3 calculations, and there are theoretical best estimates for 63 of these states.[1]

It is evident at first sight that the DFT-based methods systematically underestimate the *ab initio* reference triplet excitation energies. With one minor exception (MD of 0.02 eV of DFT/MRCI with respect to the published CASPT2 results as reference), all MDs are negative. DFT/MRCI generally fares best, for example, with regard to the theoretical best estimates (MD of −0.24 eV compared with values between −0.45 and −0.54 eV for the three TD-DFT approaches); likewise, DFT/MRCI has by far the lowest MAD (0.25 versus 0.45–0.60 eV, see Table IV). Noteworthy is also the close correspondence between DFT/MRCI and the published CASPT2 results (MD of 0.02 eV and MAD of 0.17 eV).

TABLE IV. TD-DFT and DFT/MRCI deviations of vertical excitation energies (in eV) for triplet excited states with respect to *ab initio* reference data.

	Method			
	BP86	B3LYP	BHLYP	DFT/MRCI
Published CASPT2 results[a]				
Count[b]	71	71	71	71
Mean	−0.30	−0.18	−0.19	0.02
Abs. mean	0.32	0.27	0.58	0.17
Std. dev.	0.40	0.33	0.75	0.22
Max. (+) dev.	0.26	0.65	1.85	0.69
Max. (−) dev.	0.85	0.81	1.74	0.53
MS-CASPT2/TZVP results[c]				
Count[b]	71	71	71	71
Mean	−0.56	−0.43	−0.45	−0.24
Abs. mean	0.56	0.43	0.58	0.25
Std. dev.	0.63	0.47	0.75	0.27
Max. (+) dev.	—	—	1.16	0.27
Max. (−) dev.	1.21	0.80	1.86	0.44
CC3/TZVP results[c]				
Count[b]	71	71	71	71
Mean	−0.60	−0.48	−0.49	−0.28
Abs. mean	0.60	0.48	0.60	0.28
Std. dev.	0.68	0.51	0.76	0.30
Max. (+) dev.	—	—	0.93	0.01
Max. (−) dev.	1.48	0.94	1.81	0.49
Theoretical best estimates[c]				
Count[b]	63	63	63	63
Mean	−0.53	−0.45	−0.55	−0.24
Abs. mean	0.53	0.45	0.60	0.25
Std. dev.	0.61	0.49	0.76	0.28
Max. (+) dev.	—	—	0.58	0.19
Max. (−) dev.	1.48	0.93	1.82	0.49

[a]Data from publications by the Roos group in the 1990s cited in Ref. 1.
[b]Total number of states considered.
[c]See Ref. 1.

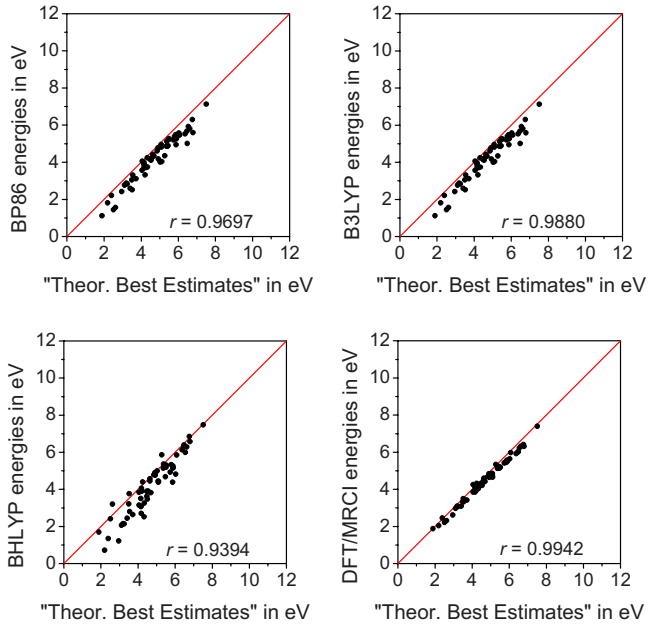

FIG. 3. (Color online) Correlation plots for all calculated triplet excited states: TD-DFT (BP86, B3LYP, and BHLYP) and DFT/MRCI vs theoretical best estimates for vertical excitation energies.

3. Excited-state energy differences

In photochemistry, the relative energies of excited states can be more important than their absolute energies. It is therefore of interest to assess the performance of the DFT-based methods also with regard to excited-state energy differences. Given their combinatorially large number, which complicates any systematic evaluation, we have decided to focus on energy differences between low-lying states that may be photochemically relevant, i.e., S_2-S_1, T_2-T_1, and S_1-T_1.

Table V presents the corresponding statistical evaluation using the best estimate energy differences as reference. We find again that DFT/MRCI performs best and TD-DFT/BHLYP performs worst. The MADs of the DFT/MRCI data for the S_2-S_1, T_2-T_1, and S_1-T_1 gaps are between 0.1 and 0.2 eV, confirming that DFT/MRCI also provides realistic energy differences. TD-DFT/BP86 and TD-DFT/B3LYP perform comparably well for the T_2-T_1 gaps, with MADs of 0.11 and 0.16 eV, in spite of the systematic underestimation of triplet excitation energies with TD-DFT (see Table IV). The S_2-S_1 energy differences are reproduced less reliably by TD-DFT/BP86 and TD-DFT/B3LYP, with MADs of about 0.4 eV and occasional reversals in the ordering of the states (six cases with TD-DFT/BP86 and five cases with TD-DFT/B3LYP). Considering the S_1-T_1 gaps, the deviations increase in the sequence DFT/MRCI < TD-DFT/BP86 < TD-DFT/B3LYP < TD-DFT/BHLYP.

4. One-electron properties

Figure 4 shows the correlation between the oscillator strengths from the current calculations and those from our previous *ab initio* study.[1] The statistical evaluation is summarized in Table VI for reference data taken from published CASPT2, MS-CASPT2/TZVP, and CC2/TZVP calculations.

Consistent with previous results,[72] the TD-DFT methods tend to underestimate the *ab initio* oscillator strengths to some extent (more so for CASPT2 or MS-CASPT2 than for CC2): The MDs are all negative and of similar magnitude as the corresponding MAD values (Table VI). The DFT/MRCI oscillator strengths are spread around the early CASPT2 reference data (MD of −0.003); they tend to be somewhat lower than the MS-CASPT2/TZVP results (MD of −0.019) and somewhat higher than the CC2/TZVP results (MD of 0.039). Considering the overall deviations in Table VI, DFT/MRCI fares best in the comparisons with the CASPT2 and MS-CASPT2/TZVP reference data, and performs similar to TD-DFT/B3LYP with respect to the CC2/TZVP data. This is also reflected in the correlation plots (Fig. 4) where DFT/MRCI shows the best correlation among the four DFT-based methods in each case, with correlation coefficients of 0.9176, 0.9493, and 0.9755 relative to CASPT2, MS-CASPT2/TZVP, and CC2/TZVP. For the sake of completeness, we note that we tested the effect of the RI approximation on the CC2/TZVP reference data and found it to be negligibly small (generally less than ±0.005 for oscillator strengths and ±0.005 eV for excitation energies).

Table VII presents the statistical evaluation for state dipole moments using early CASSCF results and the current MS-CASPT2/TZVP results as reference. The MADs of the DFT-based state dipole moments from the *ab initio* results are generally in the range between 0.6 and 0.8 D, while the corresponding MDs are considerably lower in magnitude (indicating significant scatter). Deviations of more than 1 D are

TABLE V. TD-DFT and DFT/MRCI deviations of S_2-S_1, T_2-T_1 and S_1-T_1 energy differences (in eV) with respect to theoretical best estimates.

	Method			
	BP86	B3LYP	BHLYP	DFT/MRCI
S_2-S_1 [a]				
Count[b]	27	27	27	27
Mean	−0.06	−0.03	0.02	0.04
Abs. mean	0.42	0.40	0.63	0.22
Std. dev.	0.50	0.51	0.79	0.30
Max. (+) dev.	0.98	0.82	1.32	0.91
Max. (−) dev.	1.00	1.01	1.74	0.56
T_2-T_1 [c]				
Count[b]	19	19	19	19
Mean	−0.02	0.02	0.24	−0.10
Abs. mean	0.11	0.16	0.65	0.10
Std. dev.	0.17	0.18	0.71	0.12
Max. (+) dev.	0.20	0.22	1.06	—
Max. (−) dev.	0.54	0.32	1.20	0.24
S_1-T_1 [d]				
Count[b]	20	20	20	20
Mean	0.17	0.41	1.08	0.05
Abs. mean	0.26	0.41	1.08	0.14
Std. dev.	0.27	0.48	1.29	0.19
Max. (+) dev.	0.46	0.91	2.84	0.38
Max. (−) dev.	0.25	—	0.34	0.30

[a]Energy difference between the two lowest singlet excited states.
[b]Total number of molecules considered.
[c]Energy difference between the two lowest triplet excited states.
[d]Energy difference between the lowest singlet and triplet excited states.

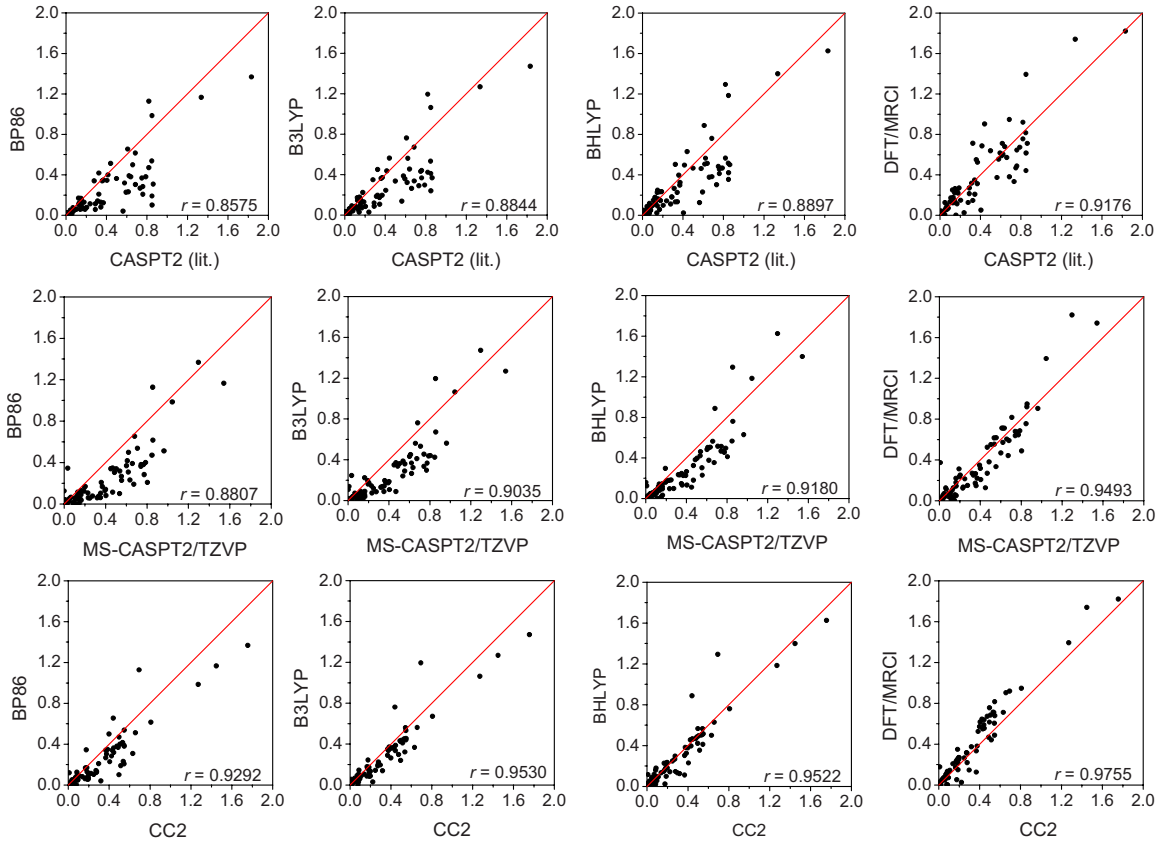

FIG. 4. (Color online) Correlation plots of oscillator strengths for all dipole-allowed excited states using earlier CASPT2, MS-CASPT2/TZVP, and CC2/TZVP results as reference data.

indeed found quite often, i.e., relative to CASSCF for 23%, 22%, 17%, and 12% of the states in TD-DFT/BP86, TD-DFT/B3LYP, TD-DFT/BHLYP, and DFT/MRCI, respectively, and relative to MS-CASPT2/TZVP for 23%, 12%, 13%, and 14% of the states (analogously).

The MDs in Table VII are all negative, which would seem to suggest that the DFT-based methods tend to give lower state dipole moments than the *ab initio* reference methods. This is deceptive insofar as the MD values are affected by a few pronounced negative outliers that occur in excited states of the nucleobases, as exemplified by the following deviations from the MS-CASPT2/TZVP dipole moments: 5 $^1A'$ state of cytosine, TD-DFT/BP86: −4.83 D; 3 $^1A''$ state of thymine, TD-DFT/B3LYP: −4.25 D; 2 $^1A'$ state of formamide, TD-DFT/BHLYP: −4.23 D; and 4 $^1A''$ state of uracil, DFT/MRCI: −4.66 D. Looking at histograms one finds that the majority of the DFT-based state dipole moments are actually larger than their *ab initio* counterparts. For example, 57%, 60%, 61%, and 57% of the state dipole moments from TD-DFT/BP86, TD-DFT/B3LYP, TD-DFT/BHLYP, and DFT/MRCI, respectively, are larger by 0–1 D than the MS-CASPT2/TZVP values.

The statistical evaluation for the dipole moments includes the ground states where the differences between DFT-based and *ab initio* results are generally smaller, with MADs ranging between 0.1 and 0.3 D, and a maximum overall deviation of 0.72 D (cytosine, TD-DFT/BHLYP versus MS-CASPT2/TZVP). Excluding the ground-state data from the statistics (18 out of 138 values) does not change the qualita-

TABLE VI. TD-DFT and DFT/MRCI deviations of oscillator strengths (in length representation) of optically allowed states with respect to *ab initio* reference data.

	Method			
	BP86	B3LYP	BHLYP	DFT/MRCI
Published CASPT2 results[a]				
Count[b]	109	109	109	109
Mean	−0.096	−0.075	−0.050	−0.003
Abs. mean	0.112	0.101	0.095	0.078
Std. dev.	0.200	0.175	0.160	0.141
Max. (+) dev.	0.307	0.375	0.473	0.543
Max. (−) dev.	0.751	0.611	0.496	0.409
MS-CASPT2/TZVP results[c]				
Count[b]	109	109	109	109
Mean	−0.112	−0.092	−0.067	−0.019
Abs. mean	0.128	0.113	0.096	0.069
Std. dev.	0.195	0.169	0.146	0.113
Max. (+) dev.	0.309	0.339	0.437	0.522
Max. (−) dev.	0.597	0.471	0.392	0.325
CC2/TZVP results[c]				
Count[b]	109	109	109	109
Mean	−0.054	−0.034	−0.009	0.039
Abs. mean	0.075	0.055	0.044	0.062
Std. dev.	0.127	0.098	0.094	0.098
Max. (+) dev.	0.433	0.501	0.599	0.290
Max. (−) dev.	0.396	0.286	0.257	0.242

[a]Data from publications by the Roos group in the 1990s cited in Ref. 1.
[b]Total number of states considered.
[c]See Ref. 1.

TABLE VII. TD-DFT and DFT/MRCI deviations of state dipole moments (in D) with respect to *ab initio* reference data.

	Method			
	BP86	B3LYP	BHLYP	DFT/MRCI
Published CASSCF results[a]				
Count[b]	138	138	138	138
Mean	−0.45	−0.39	−0.28	−0.31
Abs. mean	0.86	0.77	0.66	0.60
Std. dev.	1.38	1.25	1.05	1.09
Max. (+) dev.	2.39	2.11	1.96	1.67
Max. (−) dev.	7.11	6.39	4.80	5.86
MS-CASPT2/TZVP results[c]				
Count[b]	138	138	138	138
Mean	−0.17	−0.12	−0.01	−0.04
Abs. mean	0.75	0.59	0.61	0.58
Std. dev.	1.12	0.92	0.96	0.92
Max. (+) dev.	3.42	2.80	4.13	3.37
Max. (−) dev.	4.83	4.25	4.23	4.66

[a]Data from publications by the Roos group in the 1990s cited in Ref. 1.
[b]Total number of states considered.
[c]See Ref. 1.

tive conclusions outlined above. We have also separately considered the statistics for $n \rightarrow \pi^*$ and $\pi \rightarrow \pi^*$ excited states and seen no particular trend: Most of the statistical data are similar, and the MADs remain between 0.6 and 0.8 D for both types of excited states.

IV. SUMMARY

The statistical evaluation of the present benchmark calculations shows that DFT/MRCI performs best for vertical excitation energies, giving the lowest MADs for any of the chosen *ab initio* reference data. Within TD-DFT, the B3LYP functional is clearly superior to BP86 and BHLYP. When using the proposed theoretical best estimates for 104 singlet (63 triplet) vertical excitation energies as reference data, the MADs are 0.22 (0.25) eV for DFT/MRCI, 0.27 (0.45) eV for TD-DFT/B3LYP, 0.52 (0.53) eV for TD-DFT/BP86, and 0.50 (0.60) eV for TD-DFT/BHLYP. For singlet states, the computed excitation energies are usually in the order TD-DFT/BP86 < DFT/MRCI ≈ TD-DFT/B3LYP < TD-DFT/BHLYP, with the systematic trend that TD-DFT/BP86 (TD-DFT/BHLYP) generally underestimates (overestimates) the best estimate values. For triplet states, all studied DFT-based methods tend to give vertical excitation energies that are lower than the theoretical best estimates, with the smallest deviations for DFT/MRCI.

Concerning one-electron properties, the current comparisons are less definitive because theoretical best estimates have not yet been established for our benchmark molecules. In an overall assessment, DFT/MRCI again seems to perform best for oscillator strengths, whereas all DFT-based methods show considerable scatter for excited-state dipole moments (compared to MS-CASPT2 values obtained with the same TZVP basis). Generally speaking, the correlations between DFT-based and *ab initio* results are better for vertical excitation energies than for one-electron properties (as judged by the correlation coefficients).

The present benchmark has deliberately focused on valence excited states, such as its predecessor.[1] Low-lying valence states with double excitation character are known to be problematic for TD-DFT, and it is indeed found that the deviations for such states (e.g., in polyenes) are much larger in TD-DFT than in DFT/MRCI (which will influence but not distort the statistics). As emphasized before, the current benchmark does not include CT states and pure Rydberg states so that the statistical evaluations do not reflect the known qualitative failures of TD-DFT in these areas. It would be clearly interesting to document the performance of DFT/MRCI for these types of states, too, since the MRCI formalism should be flexible enough to treat them properly, but this is beyond the scope of the present article.

Finally, we note that a more thorough benchmarking of excited-state methods should go beyond vertical excitation spectra computed at the ground-state equilibrium geometry, by covering excited-state potential energy surfaces over a wide range of nuclear geometries (see, for example, Ref. 76). This includes proper validation of excited-state minima and conical intersections, which is essential for a reliable treatment of photochemistry. Work along these lines is in progress.

ACKNOWLEDGMENTS

M.R.S.-J. gladly acknowledges support by the Deutscher Akademischer Austausch Dienst. This work was supported by the Deutsche Forschungsgemeinschaft (SFB 663, project C4) as well as the Danish Center for Scientific Computing and the Carlsberg Foundation. We would like to thank Dr. Markus Doerr for his support with DFT/MRCI.

[1] M. Schreiber, M. R. Silva-Junior, S. P. A. Sauer, and W. Thiel, J. Chem. Phys. **128**, 134110 (2008).
[2] S. Grimme, Rev. Comput. Chem. **20**, 153 (2004).
[3] E. Runge and E. K. U. Gross, Phys. Rev. Lett. **52**, 997 (1984).
[4] A. Dreuw and M. Head-Gordon, Chem. Rev. (Washington, D.C.) **105**, 4009 (2005).
[5] R. Bauernschmitt and R. Ahlrichs, Chem. Phys. Lett. **256**, 454 (1996).
[6] F. Furche and R. Ahlrichs, J. Chem. Phys. **117**, 7433 (2002).
[7] F. Furche and R. Ahlrichs, J. Chem. Phys. **121**, 12772 (2004).
[8] D. J. Tozer, R. D. Amos, N. C. Handy, B. O. Roos, and L. Serrano-Andrés, Mol. Phys. **97**, 859 (1999).
[9] C. Adamo, G. E. Scuseria, and V. Barone, J. Chem. Phys. **111**, 2889 (1999).
[10] J. Jaramillo and G. E. Scuseria, Theor. Chim. Acta **105**, 62 (2000).
[11] J. Fabian, L. A. Diaz, G. Seifert, and T. Niehaus, J. Mol. Struct.: THEOCHEM **594**, 41 (2002).
[12] M. Parac and S. Grimme, J. Phys. Chem. A **106**, 6844 (2002).
[13] M. van Faassen and P. L. de Boeij, J. Chem. Phys. **121**, 7035 (2004).
[14] D. Jacquemin, E. A. Perpete, G. Scalmani, M. J. Frisch, R. Kobayashi, and C. Adamo, J. Chem. Phys. **126**, 144105 (2007).
[15] D. Jacquemin, E. A. Perpete, O. A. Vydrov, G. E. Scuseria, and C. Adamo, J. Chem. Phys. **127**, 094102 (2007).
[16] S. Grimme and F. Neese, J. Chem. Phys. **127**, 154116 (2007).
[17] M. J. G. Peach, P. Benfield, T. Helgaker, and D. J. Tozer, J. Chem. Phys. **128**, 044118 (2008).
[18] S. Grimme and M. Waletzke, J. Chem. Phys. **111**, 5645 (1999).
[19] S. Grimme, Chem. Phys. Lett. **259**, 128 (1996).
[20] C. Lee, W. Yang, and R. G. Parr, Phys. Rev. B **37**, 785 (1988).
[21] A. D. Becke, J. Chem. Phys. **98**, 1372 (1993).
[22] N. Gilka and C. M. Marian, J. Chem. Theory Comput. DOI:10.1021/ct8001738 (2008).

[23] A. B. J. Parusel and S. Grimme, J. Porphyr. Phthalocyanines **5**, 225 (2001).
[24] C. M. Marian, F. Schneider, M. Kleinschmidt, and J. Tatchen, Eur. Phys. J. D **20**, 357 (2002).
[25] C. Neiss, P. Saalfrank, M. Parac, and S. Grimme, J. Phys. Chem. A **107**, 140 (2003).
[26] D. Nolting, C. M. Marian, and R. Weinkauf, Phys. Chem. Chem. Phys. **6**, 2633 (2004).
[27] C. M. Marian, D. Nolting, and R. Weinkauf, Phys. Chem. Chem. Phys. **7**, 3306 (2005).
[28] C. M. Marian, J. Chem. Phys. **122**, 104314 (2005).
[29] K. A. Seefeld, C. Plutzer, D. Lowenich, T. Haber, R. Linder, K. Kleinermanns, J. Tatchen, and C. M. Marian, Phys. Chem. Chem. Phys. **7**, 3021 (2005).
[30] K. Tomić, J. Tatchen, and C. M. Marian, J. Phys. Chem. A **109**, 8410 (2005).
[31] M. Schmitt, R. Brause, C. M. Marian, S. Salzmann, and W. L. Meerts, J. Chem. Phys. **125**, 124309 (2006).
[32] C. M. Marian, J. Phys. Chem. A **111**, 1545 (2007).
[33] C. Diedrich and S. Grimme, J. Phys. Chem. A **107**, 2524 (2003).
[34] M. Schreiber, M. R. Silva-Junior, S. P. A. Sauer, and W. Thiel, J. Chem. Phys. **128**, 134110 (2008); see EPAPS Document No. E-JCPSA6-128-032811 for a literature survey on excitation energies and one-electron properties of the benchmark set. For more information on EPAPS, see http://www.aip.org/pubservs/epaps.html.
[35] A. Schäfer, C. Huber, and R. Ahlrichs, J. Chem. Phys. **100**, 5829 (1994).
[36] D. Rappoport and F. Furche, J. Am. Chem. Soc. **126**, 1277 (2004).
[37] R. Ahlrichs, M. Bär, M. Häser, H. Horn, and C. Kölmel, Chem. Phys. Lett. **162**, 165 (1989).
[38] A. D. Becke, Phys. Rev. A **38**, 3098 (1988).
[39] J. P. Perdew, Phys. Rev. B **33**, 8822 (1986).
[40] A. D. Becke, J. Chem. Phys. **98**, 5648 (1993).
[41] K. Eichkorn, O. Treutler, H. Öhm, M. Häser, and R. Ahlrichs, Chem. Phys. Lett. **242**, 652 (1995).
[42] K. Eichkorn, F. Weigend, O. Treutler, and R. Ahlrichs, Theor. Chim. Acta **97**, 119 (1997).
[43] R. Bauernschmitt and R. Ahlrichs, J. Chem. Phys. **104**, 9047 (1996).
[44] R. Bauernschmitt, M. Häser, O. Treutler, and R. Ahlrichs, Chem. Phys. Lett. **264**, 573 (1997).
[45] F. Weigend and M. Häser, Theor. Chim. Acta **97**, 331 (1997).
[46] F. Furche and D. Rappoport, *Computational Photochemistry* (Elsevier, Amsterdam, 2005), Chap. 3.
[47] M. E. Casida, in *Recent Advances in Density Functional Methods*, edited by D. P. Chong (World Scientific, Singapore, 1995), p. 155.
[48] D. Rappoport and F. Furche, J. Chem. Phys. **122**, 064105 (2005).
[49] D. J. Tozer and N. C. Handy, J. Chem. Phys. **108**, 2545 (1998).
[50] M. J. Allen and D. J. Tozer, J. Chem. Phys. **113**, 5185 (2000).
[51] A. Dreuw and M. Head-Gordon, J. Am. Chem. Soc. **126**, 4007 (2004).
[52] T. H. Dunning, Jr., J. Chem. Phys. **90**, 1007 (1989).
[53] R. A. Kendall, T. H. Dunning, Jr., and R. J. Harrison, J. Chem. Phys. **96**, 6796 (1992).
[54] See EPAPS Document No. E-JCPSA6-129-608834 for supporting information. For more information on EPAPS, see http://www.aip.org/pubservs/epaps.html.
[55] F. Weigend, M. Häser, H. Patzelt, and R. Ahlrichs, Chem. Phys. Lett. **294**, 143 (1998).
[56] C. Adamo and V. Barone, Chem. Phys. Lett. **330**, 152 (2000).
[57] R. Burcl, R. D. Amos, and N. C. Handy, Chem. Phys. Lett. **355**, 8 (2002).
[58] Z. Cai and J. Reimers, J. Phys. Chem. A **109**, 1576 (2005).
[59] M. E. Casida, C. Jamorski, K. C. Casida, and D. R. Salahub, J. Chem. Phys. **108**, 4439 (1998).
[60] R. J. Cave, F. Zhang, N. T. Maitra, and K. Burke, Chem. Phys. Lett. **389**, 39 (2004).
[61] N. C. Handy and D. J. Tozer, J. Comput. Chem. **20**, 106 (1999).
[62] C. P. Hsu, S. Hirata, and M. Head-Gordon, J. Phys. Chem. A **105**, 451 (2001).
[63] M. Shukla and J. Leszczynski, J. Comput. Chem. **25**, 768 (2004).
[64] K. B. Wiberg, A. E. de Oliveira, and G. Trucks, J. Phys. Chem. A **106**, 4192 (2002).
[65] K. Wiberg, R. Stratmann, and M. Frisch, Chem. Phys. Lett. **297**, 60 (1998).
[66] M. Barysz, A. J. Sadlej, and J. G. Snijders, Int. J. Quantum Chem. **65**, 225 (1997).
[67] N. N. Matsuzawa, A. Ishitani, D. Dixon, and T. Uda, J. Phys. Chem. A **105**, 4953 (2001).
[68] K. Nakayama, H. Nakano, and K. Hirao, Int. J. Quantum Chem. **66**, 157 (1998).
[69] P. Cronstrand, O. Christiansen, P. Norman, and H. Ågren, Phys. Chem. Chem. Phys. **2**, 5357 (2000).
[70] M. J. Paterson, O. Christiansen, F. Pawlowski, P. Jørgensen, C. Hättig, T. Helgaker, and P. Sałek, J. Chem. Phys. **124**, 054322 (2006).
[71] Y. Tawada, T. Tsuneda, S. Yanagisawa, T. Yanai, and K. Hirao, J. Chem. Phys. **120**, 8425 (2004).
[72] M. Miura, Y. Aoki, and B. Champagne, J. Chem. Phys. **127**, 084103 (2007).
[73] R. D. Amos, Chem. Phys. Lett. **364**, 612 (2002).
[74] M. Merchán and B. O. Roos, Theor. Chim. Acta **92**, 227 (1995).
[75] D. E. Freeman and W. Klemperer, J. Chem. Phys. **45**, 52 (1966).
[76] B. G. Levine, C. Ko, J. Quenneville, and T. J. Martinez, Mol. Phys. **104**, 1039 (2006).